ILKOM Jurnal Ilmiah Vol. 16, No. 1, April 2024, pp. 1-11
Accredited 2nd by RISTEKBRIN No. 200/M/KPT/2020; E-ISSN 2548-7779 | P-ISSN 2087-1716

Fall Rate Detection, Identification and Analysis Object Oriented for Elderly Safety

Sudirman Sudirman [a,b,1,*]; Ansar Suyuti [b,2]; Zahir Zainuddin [b,3]; Arief Fauzan [a,4]
[a] *Bosowa University, Jl. Urip Sumoharjo No.Km.4 Makassar and 90232, Indonesia*
[b] *Hasanuddin University, Jln. Poros Malino Km.6 Makassar and 90232, Indonesia*
[1] *sudirman.dymand@universitasbosowa.ac.id;* [2] *asuyuti06@yahoo.com;* [3] *zahir@unhas.ac.id;* [4] *arieffauzan@universitasbosowa.ac.id*
** Corresponding author*

Article history: Received April 07, 2023; Revised August 16, 2023; Accepted January 28, 2024; Available online April 26, 2024

Abstract

The aged population in Indonesia in 2021 is 30. Sixteen million people. The aged populace elderly 60 years and over reached 11.01% of the complete populace of Indonesia, which amounted to 273.88 million humans. There are ages who live on their own because of busy households with work. if there's an incident of falling elderly, a motion detection gadget is needed for monitoring the situation of the elderly at domestic. This takes a look at designing a visual synthetic intelligence hobby recognition gadget with entry from the digital camera to come across aged sports from video. take video records with the photograph Acquisition technique, Foreground Detection for changing photographs into binary, masks R-CNN to come to aware of detection items and discover the location of the incident, movement history photo, and C_motion to represent the placement of the detected object's body, SVM magnificence to categorize aged statistics falls or sports of every day residing. The experimental outcomes display that this device can come across the condensed-space version with an accuracy of ninety-seven, 50.

Keywords: Activity Recognition; Artificial Intelligence; Foreground Detection; Fall Detection; Machine Learning; Mask R-CNN; Motion History Image; Object Oriented Programming; SVM Classification.

Introduction

The elderly population in Indonesia in 2021 reached 30 million [1], constituting 11.01% of the total population of 273.88 million people [2]. Elderly residents are defined as individuals aged 60 and over [3]. Among them, 11.3 million people (37.48%) are aged 60 to 64 years, 7.77 million (25.77%) are aged 65 to 69 years, 5.1 million (16.94%) are aged 70 to 74 years, and 5.98 million (19.81%) are over 75 years old. The Ministry of Health projects that the number of elderly people will increase to 42 million (13.82%) in 2030 and further to 48.2 million (13.82%) in 2035 [4]. The rising number of elderly individuals has complex implications [5]. To address this situation, a system is required to safeguard the well-being of the aging population in Indonesia [6].

Techniques have been applied in developing a fall detection gadget, along with a tool within the shape of a sensor at the item's body, or using a camera [7]. For situations in Indonesia, fall detection the use of sensors is plenty much much less powerful, the aged memory factor is typically susceptible so the sensor has an excessive danger of being broken or out of location. Furthermore, the commonplace Indonesian populace is Muslim, so sensors will often be removed when they need to perform worship [8]. Fall detection using a digicam is one technique to stumble on the aged because it could examine the situation of gadgets without direct contact [9].

Falls because of this falls have an effect on tens of thousands and thousands of human beings around the global [10]. A maximum of the elderly's sports activities are completed at domestic, so sure places need to be watched out for. one of the most functional locations for falls to arise is the bathroom [11]. some of the results of falling, which include, weakness, and incapacity, can even grogrowe the threat of loss of life [12].

Supervision may be very critical for the elderly who have an excessive fall ability [13]. Supervision may be completed through own family participants or close human beings [14]. The character in charge of supervising is of direction required to usually be close to the aged in order that it's miles less complex to find out and offer help if the elderly revel in a fall [15]. but, as a member of the family, it isn't always possible to be across the elderly all time to carry out direct supervision [16]. consequently, supervision may be performed not directly by the use of utilizing cutting-edge era. considered one of them is applying a device that may find outfalls [17].

This gadget will detect activity reputation for tracking the condition of the aged at domestic [18]. visible artificial intelligence pastime reputation machine with enter from a camera to locate elderly hobby from video. take video

http://dx.doi.org/10.33096/ilkom.v16i1.1654.1-11

records with the photograph Acquisition method, Foreground Detection for changing images into binary, masks R-CNN to apprehend detection objects and discover the location of the incident, movement records photograph, and C_motion to symbolize the location of the detected object's frame, SVM type to categorize aged facts fall or sports of each day living [19]–[21].

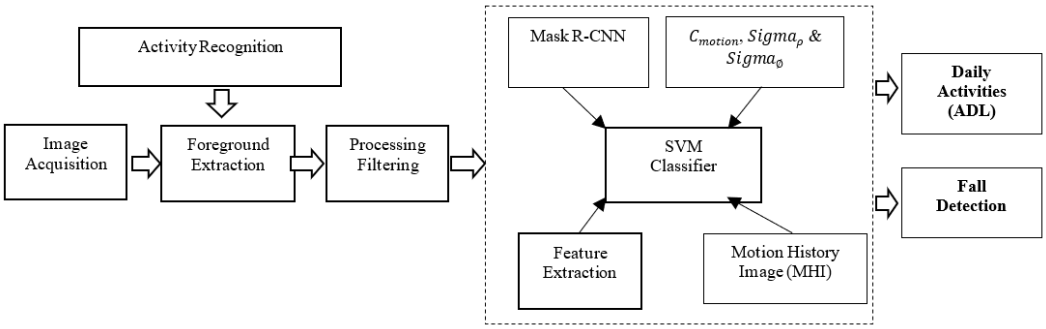

Figure 1. A Conceptual framework for Visual Artificial Intelligence Activity Recognition System Elderly for Identification, Pattern Recognition and Analysis. Source: Author's elaboration.

A. Image Acquisition

Digital photograph acquisition is the manner of shooting or scanning analog photographs to obtain virtual photo facts. The input of this autumn detection system is the recorded video statistics. Video information is entered into records for fall detection using CCTV cameras.

$$Gleam = \frac{1}{3}(R' + G' + B') \quad (1)$$

The system of changing the RGB fee of each pixel in a photograph right into an unmarried (eight-bit) value with several zero-255. The picture effects produced with the aid of the colour-to-grayscale technique include gravy, which has variations in black at the weakest depth and white at the strongest depth. virtual image acquisition is the manner of shooting or scanning analog pix to gain a virtual photo. The input of this autumn detection device is the recorded video records.

B. Foreground Extraction

The process of isolating the desired item. Foreground detection is an image processing method that separates items from the historical past. The result of this detection is a binary photo in which the detected item has a pixel fee of 1 (White) at the same time as the history around the item has a pixel price of 0 (black) [22], [23].

C. Processing Filtering

Gets rid of some noise inside the preceding foreground image, so that a few white dots inside the photograph disappear.

D. Feature Extraction

Each item is extracted with its characteristics based totally on positive parameters and grouped in certain instructions. traits that may be used to differentiate one object from some other encompass shape traits, length traits, geometric traits, texture characteristics, and color characteristics as enter facts inside the identity/classification method.

E. Foreground Detection

The procedure of separating the favored item (foreground) from different unwanted objects (historical past), specifically converting the picture into the binary, binary image where the detected item has a pixel price of 1 (White) whilst the heritage across the item has a pixel fee of zero (black).

$L \leftarrow 0; Z \leftarrow \emptyset wen\ t = 1 x_t = (R, G, B), I$

$\leftarrow \sqrt{R^2 + G^2 + B^2 if} = colordist(X_t, V_m) \geq \in_1 if$

$= brightnes(\langle I, \check{I}_m, \hat{I}_m \rangle)$ Searching the codeword

$= c_1 in\ \xi = \{c_2, c_2, \ldots, c_n$ to match $x_t if = z \leftarrow \emptyset$

= n matching codeword L

$\leftarrow l + 1$ and new codeword $C_i V_i \leftarrow aux_l$

$\leftarrow \langle I, I, 1, t-1, t, t\rangle$ rest matching codeword

$= C_1$ including $V_m = (R_m, G_m, B_m)$ and aux_m

$= \langle I_m, \hat{I}_m, \lambda_m, p_m, q_m\rangle v_m$

$\leftarrow \left(\frac{F_m R_m + R}{f_m + 1}, \frac{F_m G_m + G}{f_m + 1}, \frac{F_m B_m + B}{f_m + 1} aux_m\right)$

$\leftarrow \langle \min\{I, I_m\}, \max\{I, I_m\}, F_m + 1, \max\{\lambda_m, t - q_m\}, p_m, t\rangle$

Maximum time interval = $c_1(i = 1)$ qualmatched pixels = $\lambda_1 \leftarrow \max\{\lambda_i, (n - q_1 + p_1 - 1)\}$ pixel $x_t = (R, G, B)$ and codeword $c_1, v_1 = (R_i, G_i, B_i)$, exiting; $||X_t||^2 R^2 + G^2 + B^2 \left||v_i|\right|^2 \leq \bar{R}_i^2 + \bar{G}_i^2 + \bar{B}_i^2$

$(x_t, v_t)^2 = (\bar{R}_i R + \bar{G}_i G + \bar{B}_i B)^2$

Colordist $(x_t, v_t) = p^2 = \left||X_t|\right|^2 \cos^2 \emptyset = \frac{(x_t, v_t)^2}{\left||v_i|\right|^2}$

Colordist $(x_t, v_t) = \delta = \sqrt{\left||X_t|\right|^2 - p^2}$

Figure 2. Foreground detection. Source: Author's elaboration.

F. Motion History Image (MHI)

Movement history photo has constructed the usage of previously filtered images, then the photograph is used as enter records to assemble MHI. Motion records photo is an photograph processing approach to come across object motion, this method detects motion based totally on pixel modifications. The movement of the object is taken from a video that has been divided into numerous series pix. To gain MHI, step one is to extract the binary motion sequence of the object D(x,y,t) from the specific photograph I(x,y,t) using the photograph-differencing method [24], [25]. Then every pixel of the movement records photo Ht is a function within the time range t (1 τ n), the Equation 2 is:

$$H_t(x, y, t) = \int_{\max(0, H_t(x,y,t-1)-1)}^{t} ifD(x, y, t) = 1 \quad (2)$$

X = Pixel position at coordinates x.
Y = The position of the pixel on the y coordinate.
$H\tau(x, y, t)$ = *Motion History Image* (MHI).
$D(x, y, t)$ = Binary sequence of object movements.

Photo information can be processed the usage of the set of rules in Equation 1 to produce an MHI picture as shown in **Figure 3**.

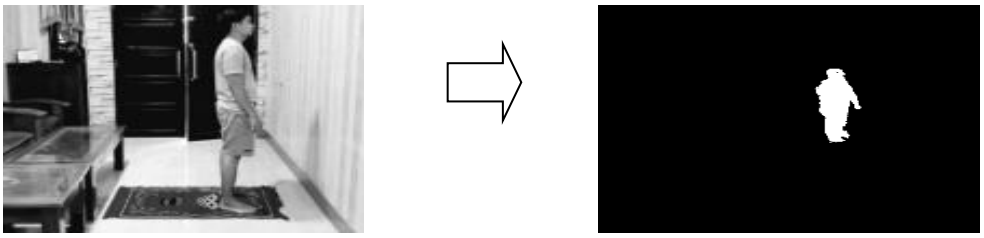

Figure 3. Motion History Image (MHI) image results. Source: Author's elaboration.

G. Looking for values ρ and θ

After you have the MHI, the subsequent step is to discover the theta and rho values, those values constitute the placement of the detected object frame. To get the theta value is to apply Equation 3.

$$\emptyset \frac{1}{2}\tan^{-1}\left(\frac{2\mu 11}{\mu 20-\mu 02}\right) \quad (3)$$

$\emptyset = Ellipse\ orientation$

While to get the value of rho is to use Equation 4.

$$\rho \frac{a}{b} \quad (4)$$

a: Major semi-axis a.
b: Minor semi-axis b.
ρ: Ratio ellipse.

H. Values C_{motion}, $sigma_\rho$ and $sigma_\emptyset$

Look for the values of C_{motion}, $sigma_\rho$, and $sigma_\emptyset$. The values of these 3 parameters represent the motion and position of the item's frame so that the ones 3 parameters could be used as a reference for the fall detection system on the item. The C_motion parameter represents the velocity of the item's motion it's given a scale of 0-100, wherein zero way still and 100 manner entire motion. To calculate the charge of C_motion is to use the following Equation 5.

$$C_{motion} = \frac{\sum pixel_{x,y}\ \in blob\ H_\tau\ (x,y,t)}{\#pixels \in blob} \quad (5)$$

C_{motion}= Percentage of object movement.
$Blob$ = Pixels that represent objects

After calculating C_{motion}, $sigma_R$ and $sigma_\emptyset$ are calculated, in those values are acquired from the subsequent Equation 6 and 7.

$$sigma_\emptyset = \sigma\emptyset \quad (6)$$
$$sigma_\rho = \sigma\emptyset \quad (7)$$

$Sigma_\emptyset$ = The standard deviation of the theta value.
$Sigma_\rho$ = Standard deviation of the rho value.

I. Approximated Ellipse

The alternate in inclination perspective can distinguish squatting and falling well, whilst the elderly squat, the angle will not alternate a lot, but when the elderly fall, the body changes might be vertical to horizontal, and the perspective will change lot. items might be expected the use of an ellipse the usage of moments. An ellipse is defined through the centroid (x,y), orientation, and predominant semi-axis a and minor semi-axis b [26], [27].
For a non-stop photograph, the moment's fee is acquired from:

$$m_{pg} = \int_{-\infty}^{\infty}\int_{-\infty}^{\infty} x^p\, y^p f(x,y)dxdy \quad (8)$$

mpq = Moments Value
value $i\ p,q$ = 0,1,2

The centroid of the ellipse is obtained by calculating the coordinates of the middle of mass with first and 0 spatial order moments:

$$\bar{x} = \frac{m10}{m00}; \bar{y} = \frac{m01}{m00}; \quad (9)$$

x = Centroid on the x-axis coordinates.
y = Centroid on the y-axis coordinates.

Centroid (x,y) is used to calculate the primary moments:

$$\mu_{pq} = \int_{-\infty}^{\infty}\int_{-\infty}^{\infty} (x-\bar{x})^p\ (y-\bar{y})^q f(x,y)dxdy \quad (10)$$

μpq = Central moments.

The attitude among the item's foremost axis and the horizontal x-axis offers the orientation of the ellipse, and can be calculated through central moments of order 2:

$$\emptyset = \frac{1}{2}\ tan^{-2}(\frac{2\mu_{11}}{\mu_{20}-\mu_{02}}) \quad (11)$$

$\emptyset$ = Ellipse orientation.
To get the major semi-axis a and the minor semi-axis b from the ellipse, we must calculate Imin and Imax, specifically the smallest second of inertia and the biggest moment of inertia [28], [29]. This price can be calculated via evaluating the eigenvalues of the covariance matrix:

$$J = \begin{pmatrix} \mu_{20} & \mu_{11} \\ \mu_{11} & \mu_{11} \end{pmatrix} \quad (12)$$

The eigenvalues of the J matrix are Imin and Imax that are calculated by

$$I_{min} = \mu_{20} + \mu_{20} - \frac{\sqrt{(\mu_{20} - \mu_{02})^2 + 4\mu_{11^2}}}{2}$$
$$I_{max} = \mu_{20} + \mu_{20} - \frac{\sqrt{(\mu_{20} - \mu_{02})^2 + 4\mu_{11^2}}}{2} \quad (13)$$

J = covariance matrix.
I_{min} = The smallest moment of inertia.
I_{max} = The greatest moment of inertia

Then the most important semi-axis a and minor semi-axis b of the ellipse are:

$$a = (\frac{4}{\pi})^{\frac{1}{4}} \left(\frac{(I_{\max})^3}{I_{min}} \right)^{1/8}$$
$$a = (\frac{4}{\pi})^{\frac{1}{4}} \left(\frac{(I_{\min})^3}{I_{max}} \right)^{1/8} \quad (14)$$

And to decide the ratio of the ellipse:

$$\rho \frac{a}{b} \quad (15)$$

a = *Major semi-axis* a
b = *Minor semi-axis* b
ρ = Ellipse ratio

J. Support Vector Machine (SVM)

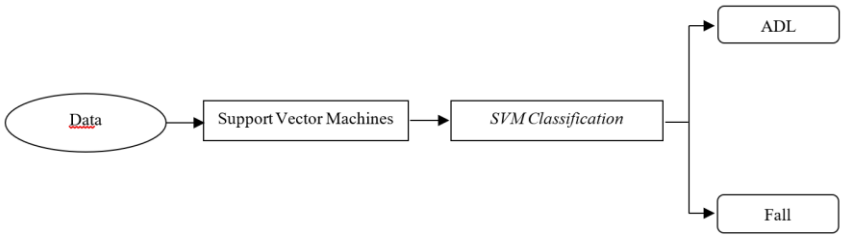

Figure 4. Support Vector Machine (SVM)—source: Author's elaboration.

The SVM layout makes use of stages to assess the posture of the elderly. the first level classification assesses whether the old person is standing, while the end result suggests the old man isn't status, putting him within the 2nd stage classifier. At this stage, judging whether the elderly have fallen, we discover the elderly have fallen, the machine will have an alarm.

$$y9x) = w^T \emptyset(X) + b \quad (16)$$

In which x is the input vector, w is the load parameter, (X) is the basis feature, and b is a bias, due to the fact squatting and falling have comparable features, the second one-order classifier distinguishes squats and falls. makes use of 4 features: the ratio of the essential and minor axes of the ellipse, the task region of the shifting object, the angle of inclination of the ellipse, the tendency of variant of the important and minor axes. The projection region represents the quantity of non-zero moving pixels within the transferring object after binarization. while squatting, the elderly will lift his body and the venture vicinity might be small, while he falls, the frame will stretch, the location may be larger. So, it's miles used to distinguish squat and fall.

A. Mask R-CNN

The R-CNN mask is used to solve the example segmentation problem. inside the mask R-CNN set of rules, a brand-new layer for predicting the segmentation mask of every place of interest (ROI) runs in parallel with the layer for classification and bounding field regression.

Region proposal network (RPN), that is a short search for feasible object locations from an enter image. The possible positions of items within the photograph are then given a boundary and marked as vicinity of interest (ROI). RPN then takes sub-snap shots of viable gadgets of various sizes as input into the Convolutional Neural community

with output a set of rectangles with object similarity scores. Prediction of class (class) and box offset (regression) in parallel from possible objects. From this step, mask R-CNN additionally outputs a binary mask for each RoI.

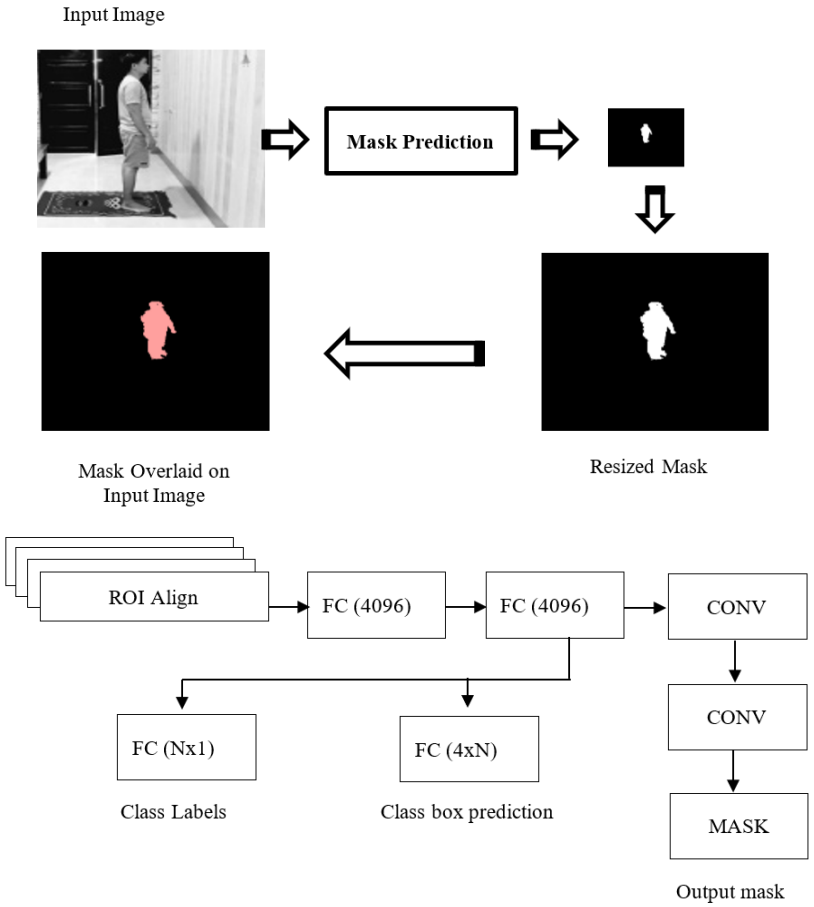

Figure 5. Mask R-CNN. **Source:** Author's elaboration. Source: Author's elaboration.

The key element of mask R-CNN is pixel-to-pixel alignment, which is a major lacking a part of rapid/faster R-CNN. mask R-CNN adopts the same two-degree method with an identical first level. inside the 2nd level, in parallel to predicting the class and offset of the container, masks R-CNN also outputs binary masks for every RoI. this is in comparison to the state-of-the-art machine, in which classification is based on mask predictions.

R-CNN masks are implemented and educated due to the faster R-CNN framework, which enables various bendy architectural designs. in addition, the mask branch adds most effective a small computational overhead, permitting fast systems and fast experiments [30], [31].

To get the most appropriate model, and to test a system, of course, in terms of its use, use the R-CNN method. From the tests carried out from the previous method, several things are considered in selecting the best method. Related research regarding the use of video as input data requires heavy computation so supporting hardware is needed.

Several things need to be considered in choosing an R-CNN method, low power consumption by recognizing the detected object. low computational work, has a fast response can respond well to almost all computing processes, and the speed of sending fall detector data has an average of 10.9 seconds in 10 trials. Better performance outperforms previous studies which reached 95-98.7%.

Results and Discussion

$$\text{Accuracy}\frac{TP+TN}{TP+FP+TN+FN} \quad (17)$$

Actual advantageous (TP), the device circumstance detects as falling activity, while the interest falls. true poor (TN), the circumstance the device detects as a hobby does not fall when the pastime does now not fall. false wonderful (FP), the condition the gadget detects as falling hobby when the pastime does not fall. fake terrible (FN), the circumstance the machine detects as a non-falling interest, while the activity falls.

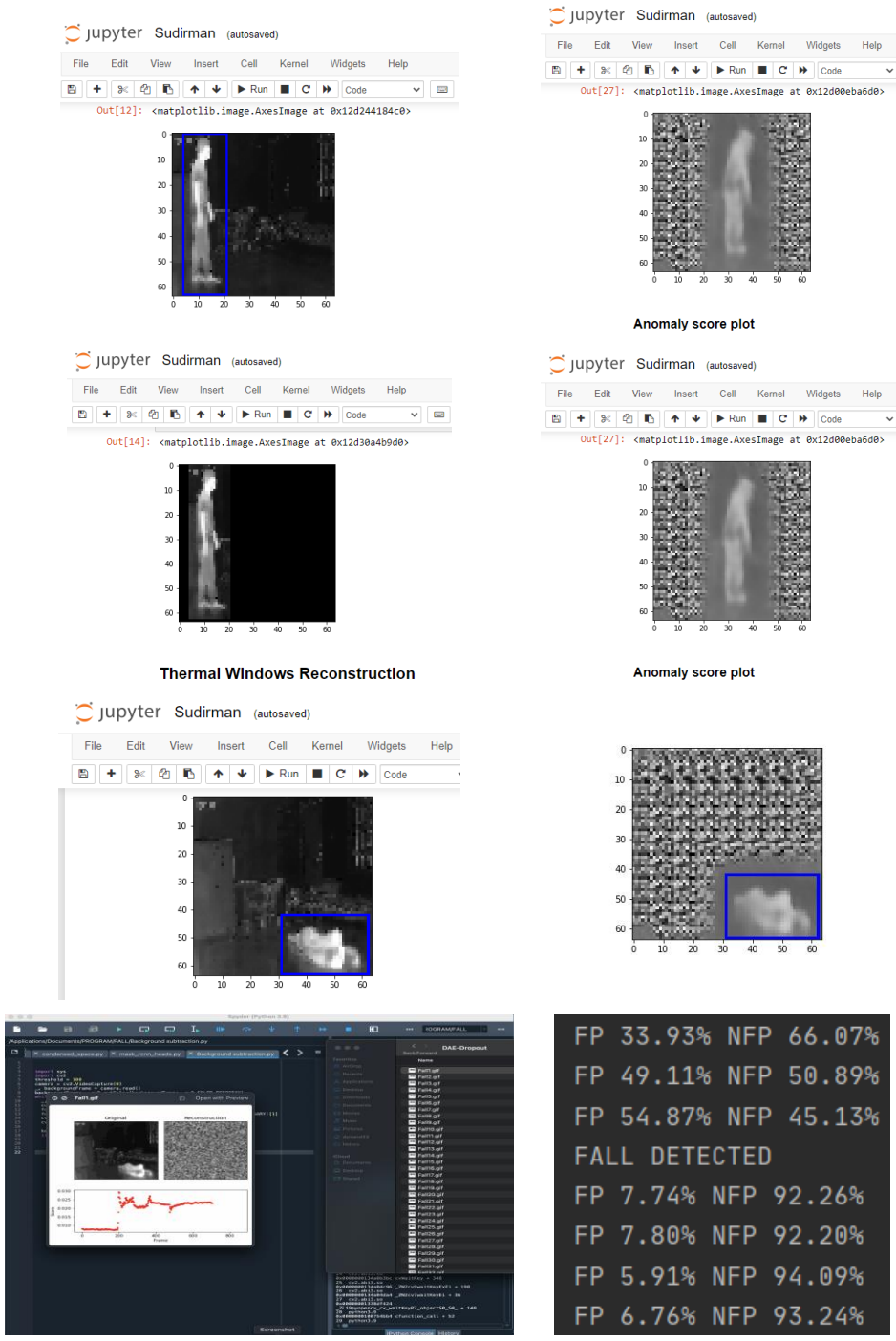

Figure 6. Falls results—source: Author's elaboration.

This take a look at makes use of PyTorch that's educated the use of a fall detection dataset. Fall detection assessments and daily sports are executed in numerous locations, along with the Unhas CBS Lab, Unhas IOT LAB, classroom, office Room, and domestic. The model schooling uses 70% training, 20% validation, and 10% take a look at techniques. within the trying out section, a total of 1458 samples with an accuracy of ninety-seven.4% (1420/1458). The model became loaded into Python the use of OpenCV, a dataset used with a complete of 142 crash films and 154 ADL videos. All samples were utilized in each fashion. then examined the ambitious-spaced model. After that, 142 movies crashed and 154 ADLs were processed by the normal version. The consequences are calculated and offered below for the everyday model and the compact-spaced version:

A. Accuracy for Fall

They were using two experimental accuracy models, namely the condensed-space model and the Regular model. With the number of experimental data of 4 cameras, camera 0, the number of successful 39 data, and the number of Testing 40 data with an accuracy of 97.5%. Camera data 1 34 was successful from 35 tests to an accuracy of 97.14.

Camera 2 was successful in 36 out of 37 trials. Camera 3 29 successes out of 30 tries. A total of 138 trials of 142 trials resulted in an accuracy of 97.15%.

The camera's Regular Accuracy Model 0 produced 39 successes out of 40 trials resulting in an Accuracy of 97.50. Camera 1 produced 33 successes out of 35 trials resulting in an accuracy of 94.29%. Camera 2 data succeeded in 33 out of 35 trials producing 94.59% accuracy. And camera 3 succeeded 29 out of 30 trials resulting in 96.67% Accuracy. The total successful data of 136 out of 142 trials resulted in an accuracy of 95.76%.

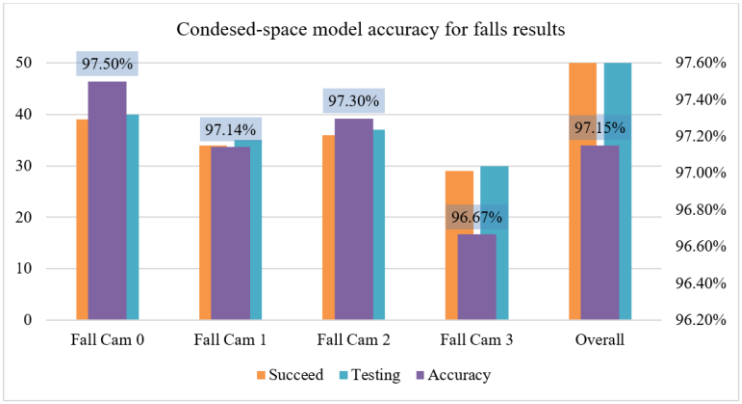

Figure 7. Condensed-space model accuracy for fall results

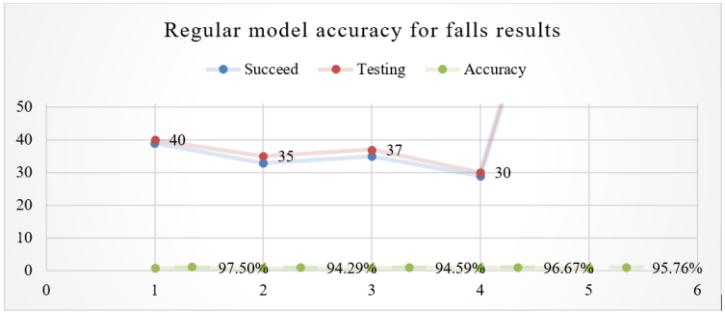

Figure 8. Regular model accuracy for fall results

B. Accuracy for ADL

Using two models of accuracy in the Daily Activities of the Elderly, namely the Condesed-space model. With the number of experimental data 4 cameras, camera 0, the number of successes 39 data from the number of trials 40 data with an accuracy of 97.50%. Camera data 1.37 was successful from 38 experiments so the accuracy was 97.37%. Camera 2 i.e. 38 successful out of 39 trials Produced 97.37% Accuracy. Camera 3, 36 success out of 37 trials Yield 97.30%. A total of 150 trials of 154 trials resulted in an accuracy of 97.40%.

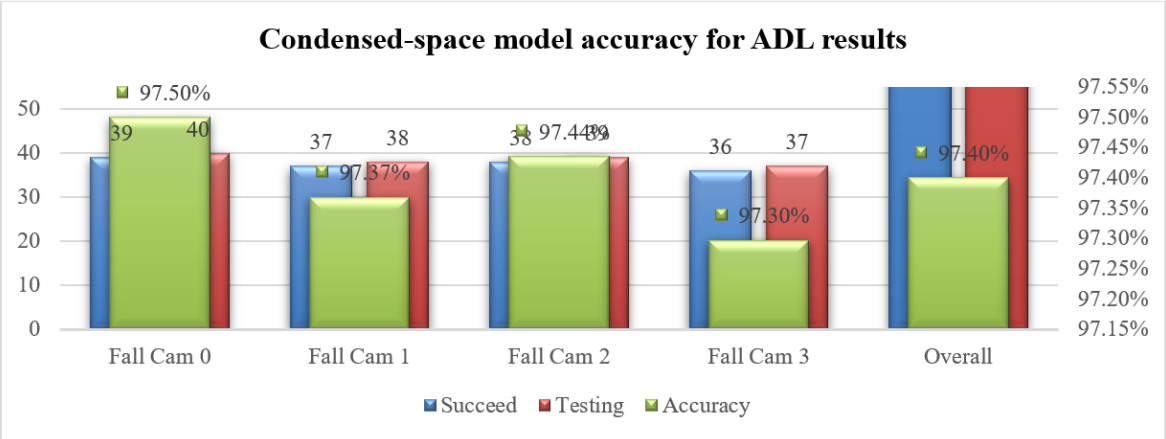

Figure 9. Condensed-space model accuracy for ADL results

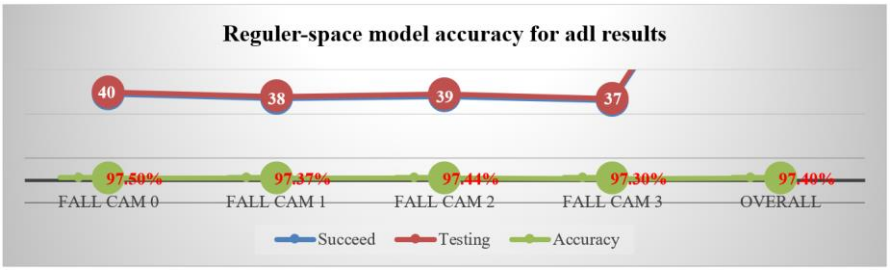

Figure 10. Regular-space model accuracy for ADL results

C. Performance

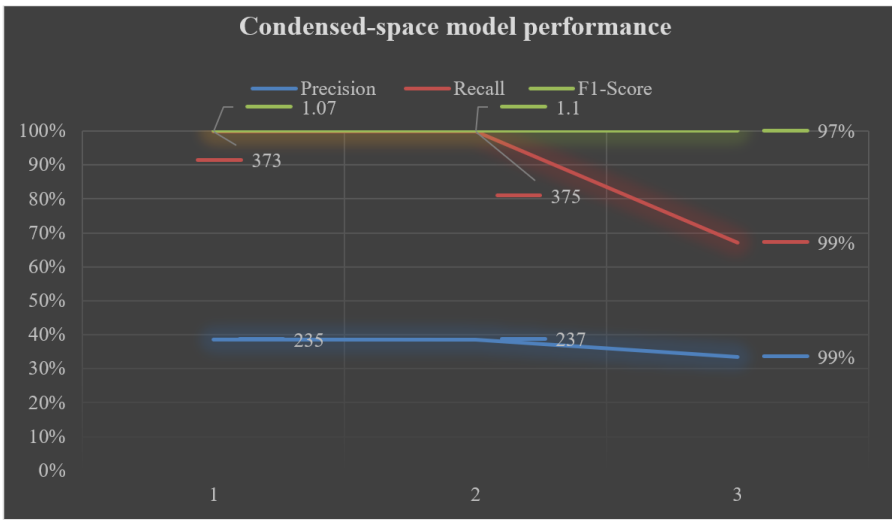

Figure 11. Condensed-space model performance

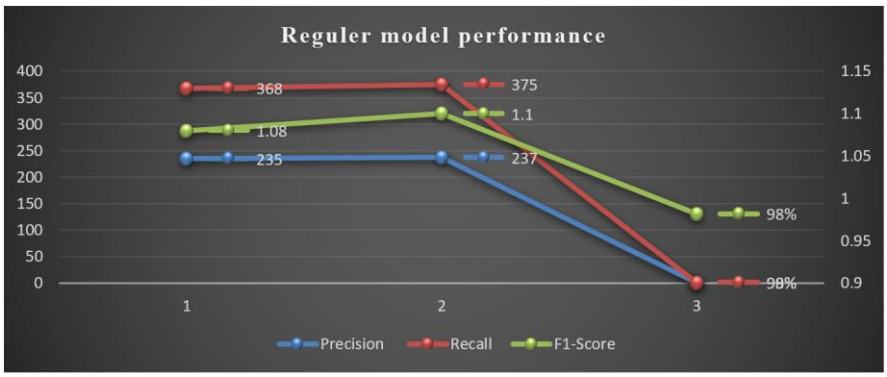

Figure 12. Reguler model performance

As inside the desk above, the condensed-spaced version has an overall accuracy of 98. forty% regarding fall detection. The difference among better and decrease accuracy scores is because of several primary motives. First, the edge cost can be set within the variety, of 0.1 – zero. five, which offers distinctive consequences. some of the reasons for this score are ADL video progress from everyday brightness, to dim, to complete darkness.

Conclusion

Visual synthetic intelligence hobby recognition gadget with input from the digicam to come across elderly activities from the video is one technique to discover objects due to the fact it may analyse the situation of items without direct touch. fall detection machine Makes it simpler to stumble on movement, in particular falling moves in each day sports finished by way of the elderly, makes it simpler for a circle of relatives' individuals to get facts while the aged falls and Assists in accepting the region of falls in the elderly when they fall.

Acknowledgment

We thank Zahir Zainduddin for coordinating every activity in this research, conducting pre-tests and post-tests and analyzing the programming and facilities of each laboratory activity.

References

[1] R. Sekartaji *et al.*, 'Dietary diversity and associated factors among children aged 6–23 months in Indonesia', *J Pediatr Nurs*, vol. 56, 2021, doi: 10.1016/j.pedn.2020.10.006.

[2] L. Jia *et al.*, 'Prevalence, risk factors, and management of dementia and mild cognitive impairment in adults aged 60 years or older in China: a cross-sectional study', *Lancet Public Health*, vol. 5, no. 12, 2020, doi: 10.1016/S2468-2667(20)30185-7.

[3] R. Tosepu *et al.*, 'Correlation between weather and Covid-19 pandemic in Jakarta, Indonesia', *Science of the Total Environment*, vol. 725, 2020, doi: 10.1016/j.scitotenv.2020.138436.

[4] A. Orben, L. Tomova, and S. J. Blakemore, 'The effects of social deprivation on adolescent development and mental health', *The Lancet Child and Adolescent Health*, vol. 4, no. 8. 2020. doi: 10.1016/S2352-4642(20)30186-3.

[5] G. Das Mahapatra, S. Mori, and R. Nomura, 'Reviewing the Universal Mobility of the Footpaths in the Centers of Historic Indian Cities through Field Survey', *Sustainability (Switzerland)*, vol. 15, no. 10, 2023, doi: 10.3390/su15108039.

[6] E. Yulianto, P. Utari, and I. A. Satyawan, 'Communication technology support in disaster-prone areas: Case study of earthquake, tsunami and liquefaction in Palu, Indonesia', *International Journal of Disaster Risk Reduction*, vol. 45, 2020, doi: 10.1016/j.ijdrr.2019.101457.

[7] D. Mrozek, A. Koczur, and B. Małysiak-Mrozek, 'Fall detection in older adults with mobile IoT devices and machine learning in the cloud and on the edge', *Inf Sci (N Y)*, vol. 537, 2020, doi: 10.1016/j.ins.2020.05.070.

[8] Q. Feng, C. Gao, L. Wang, Y. Zhao, T. Song, and Q. Li, 'Spatio-temporal fall event detection in complex scenes using attention guided LSTM', *Pattern Recognit Lett*, vol. 130, 2020, doi: 10.1016/j.patrec.2018.08.031.

[9] M. Al Duhayyim, 'Automated disabled people fall detection using cuckoo search with mobile networks', *Intelligent Automation and Soft Computing*, vol. 36, no. 3, 2023, doi: 10.32604/iasc.2023.033585.

[10] F. Y. Qin, Z. Q. Lv, D. N. Wang, B. Hu, and C. Wu, 'Health status prediction for the elderly based on machine learning', *Arch Gerontol Geriatr*, vol. 90, 2020, doi: 10.1016/j.archger.2020.104121.

[11] G. Afuwai, K. M. Lawal, P. Sule, and A. E. Ikpokonte, 'Interpretation of Geoelectric Pseudo-Section of a Profile Across a Functional Borehole Located In-between Two Non-Functional Dug-Wells', *Journal of Environment and Earth Science*, vol. 5, no. 17, 2015.

[12] J. A. Woods *et al.*, 'The COVID-19 pandemic and physical activity', *Sports Medicine and Health Science*, vol. 2, no. 2. 2020. doi: 10.1016/j.smhs.2020.05.006.

[13] L. Arnau-Sabatés, A. Dworsky, J. Sala-Roca, and M. E. Courtney, 'Supporting youth transitioning from state care into adulthood in Illinois and Catalonia: Lessons from a cross-national comparison', *Child Youth Serv Rev*, vol. 120, 2021, doi: 10.1016/j.childyouth.2020.105755.

[14] C. A. Pelletier, K. Cornish, and C. Sanders, 'Children's independent mobility and physical activity during the covid-19 pandemic: A qualitative study with families', *Int J Environ Res Public Health*, vol. 18, no. 9, 2021, doi: 10.3390/ijerph18094481.

[15] Y. Xu, X. Yan, X. Liu, and X. Zhao, 'Identifying key factors associated with ridesplitting adoption rate and modeling their nonlinear relationships', *Transp Res Part A Policy Pract*, vol. 144, 2021, doi: 10.1016/j.tra.2020.12.005.

[16] M. Porumb, C. Griffen, J. Hattersley, and L. Pecchia, 'Nocturnal low glucose detection in healthy elderly from one-lead ECG using convolutional denoising autoencoders', *Biomed Signal Process Control*, vol. 62, 2020, doi: 10.1016/j.bspc.2020.102054.

[17] S. Saha, S. Deb, and P. P. Bandyopadhyay, 'Precise measurement of worn-out tool diameter using cutting edge features during progressive wear analysis in micro-milling', *Wear*, vol. 488–489, 2022, doi: 10.1016/j.wear.2021.204169.

[18] R. S. Chandel, S. Sharma, S. Kaur, S. Singh, and R. Kumar, 'Smart watches: A review of evolution in bio-medical sector', in *Materials Today: Proceedings*, 2021. doi: 10.1016/j.matpr.2021.07.460.

[19] X. Xu *et al.*, 'Crack Detection and Comparison Study Based on Faster R-CNN and Mask R-CNN', *Sensors*, vol. 22, no. 3, 2022, doi: 10.3390/s22031215.

[20] A. Pampouchidou *et al.*, 'Quantitative comparison of motion history image variants for video-based depression assessment', *EURASIP J Image Video Process*, vol. 2017, no. 1, 2017, doi: 10.1186/s13640-017-0212-3.

[21] M. A. Haziq Megat S'Adan, A. Pampouchidou, and F. Meriaudeau, 'Deep Learning Techniques for Depression Assessment', in *International Conference on Intelligent and Advanced System, ICIAS 2018*, 2018. doi: 10.1109/ICIAS.2018.8540634.

[22] Y. Zhang, L. Yu, S. Li, G. Wang, X. Jiang, and W. Li, 'The Extraction of Foreground Regions of the Moving Objects Based on Spatio-Temporal Information under a Static Camera', *Electronics (Switzerland)*, vol. 12, no. 15, 2023, doi: 10.3390/electronics12153346.

[23] Y. Tang, Y. Wang, and Y. Qian, 'Railroad Crossing Surveillance and Foreground Extraction Network: Weakly Supervised Artificial-Intelligence Approach', *Transp Res Rec*, vol. 2677, no. 9, 2023, doi: 10.1177/03611981231159406.

[24] D. M. Tsai, W. Y. Chiu, and M. H. Lee, 'Optical flow-motion history image (OF-MHI) for action recognition', *Signal Image Video Process*, vol. 9, no. 8, 2015, doi: 10.1007/s11760-014-0677-9.

[25] Sudirman, 'Konferensi Nasional Ilmu Komputer (KONIK) 2021 Machine Learning Deteksi Jatuh Menggunakan Algoritma Human Posture Recognition', *Konferensi Nasional Ilmu Komputer (KONIK)*, 2021.

[26] H. Feng and J. Liang, 'A modified stable node-based smoothed finite element method based on low-quality unstructured mesh', *Eng Anal Bound Elem*, vol. 150, 2023, doi: 10.1016/j.enganabound.2023.02.037.

[27] F. Yoshida *et al.*, 'Multi-chord observation of stellar occultation by the near-Earth asteroid (3200) Phaethon on 2021 October 3 (UTC) with very high accuracy', *Publications of the Astronomical Society of Japan*, vol. 75, no. 1, 2023, doi: 10.1093/pasj/psac096.

[28] M. Menozzi, A. v. Buol, H. Krueger, Ch. Miège, and C. Pedrono, 'Fitting Varifocal Lenses: Strain as a Function of the Orientation of the Eyes', 2023. doi: 10.1364/ovo.1992.thd1.

[29] X. Feng, S. Gao, Y. Song, Z. Hu, L. Chen, and T. Liang, 'Static and Dynamic Analysis of Conductor Rail with Large Cross-Sectional Moment of Inertia in Rigid Catenary Systems', *Energies (Basel)*, vol. 16, no. 4, 2023, doi: 10.3390/en16041810.

[30] R. Rijayanti, M. Hwang, and K. Jin, 'Detection of Anomalous Behavior of Manufacturing Workers Using Deep Learning-Based Recognition of Human–Object Interaction', *Applied Sciences (Switzerland)*, vol. 13, no. 15, 2023, doi: 10.3390/app13158584.

[31] T. Kasinathan and S. R. Uyyala, 'Detection of fall armyworm (spodoptera frugiperda) in field crops based on mask R-CNN', *Signal Image Video Process*, vol. 17, no. 6, 2023, doi: 10.1007/s11760-023-02485-3.